

Multi-ion fluid simulation of tokamak edge plasmas including non-diffusive anomalous cross-field transport

A.Yu. Pigarov^{a,*}, E.M. Hollmann^a, S.I. Krasheninnikov^a,
T.D. Rognlien^b, W.P. West^c

^a University of California at San Diego, EBU-II, 9500 Gilman Dr., La Jolla, CA 9209-0417, USA

^b Lawrence Livermore National Laboratory, Livermore CA, USA

^c General Atomics, P.O. Box 85608, San Diego, CA, USA

Abstract

The two-dimensional, multi-ion, fluid code UEDGE is used to simulate the sophisticated transport of impurities in the tokamak edge plasma. The UEDGE model incorporates the effects of non-diffusive intermittent cross-field transport by using anomalous convective velocities whose spatial profile is adjusted for each ion charge state to match available experimental data. The simulations of low-confinement (L-mode) shots indicate that: (i) anomalous convective transport dominates in the far scrape-off layer; (ii) different impurity charge states have different magnitudes and signs in their convective velocities; and (iii) chamber wall sputtering is an important source of impurities.

© 2004 Elsevier B.V. All rights reserved.

PACS: 52.55.Fa; 52.65.Kj

Keywords: Edge plasma; Impurity transport; UEDGE, DIII-D; Intermittent transport

1. Introduction

Recent experimental and theoretical studies have shown that fast intermittent cross-field plasma transport can play the dominant role in the scrape-off layer (SOL) of many tokamaks (see Refs. [1,2] and literature cited therein). This kind of transport is associated with coherent structures (blobs) that separate from core plasma and propagate outward, i.e., the transport is convective rather than diffusive. The resulting convective plasma

flux to the chamber wall enhances the recycling of neutral particles in the main chamber and increases impurity production via physical, chemical, and self-sputtering. Moreover, it is thought that other coherent structures (holes) corresponding to density depressions could propagate into the core plasma. The intermittent non-diffusive transport associated with these holes could enhance impurity ion transport and cause significant core plasma contamination.

The edge plasma physics code UEDGE [3] has been used to simulate impurity transport including anomalous intermittent cross-field convection (AICFC) for impurity and main plasma ions [4,5]. This paper presents results on further validation of the AICFC model against experimental data on carbon impurity profiles.

* Corresponding author. Tel.: +1 858 822 4916; fax: +1 858 534 7716.

E-mail address: apigarov@uscg.edu (A.Yu. Pigarov).

2. The AICFC model

In the AICFC model incorporated into the UEDGE code, the 2D profile of convective cross-field velocity has the following form: $V_{\text{conv}}(\psi_N, \theta, Z) = V_{\text{BPconv}}(\psi_N, \theta) A_s(Z)$. Here the profile is given in magnetic flux surface coordinates (ψ_N and θ), where ψ_N is the normalized poloidal magnetic flux, θ is viewed as the poloidal coordinate, $V_{\text{BPconv}}(\psi_N, \theta)$ is the AICFC velocity of the dominant background species, and the $A_s(Z)$ is the relative amplitude factor for each charge state Z of ion species s . The amplitude factors vary in the range; $-1 \leq A_s(Z) \leq +1$. For the deuterium background ions, $s = \text{D}^+$, we have $A_s(Z) \equiv 1$ and $V_{\text{conv}} \equiv V_{\text{BPconv}}$. The $V_{\text{BPconv}}(\psi_N, \theta)$ profile has been discussed in Ref. [5]. The V_{BPconv} strongly increases with minor radius (i.e., with ψ_N) and has maximum in θ -direction at the outer mid-plane.

The positive amplitude factors correspond to charge states of impurity ions that are convected toward the wall with non-diffusive transport dominated by plasma density blobs. By contrast, the negative amplitude factors correspond to the charge states of impurities which are dominantly entrained in inwardly moving plasma density holes. In general, the amplitude factors are independent parameters. The set of values of amplitude factors for all charge state of the impurity species studied here (i.e., of carbon C^{Z+} , $Z = 1-6$, $s = \text{C}$) is assumed to increase monotonically with increasing Z , i.e., $A_C(\text{C}^{Z+}) > A_C(\text{C}^{(Z-1)+})$. The highest impurity charge states are thought to behave more like the background plasma ions, so in the paper, we use $A_C(6) = 1$ for the fully stripped carbon ion. For convenience of discussion, the set of amplitude factors is characterized by the single parameter $\eta_{\text{CC}} = A_C(1) + A_C(2) + A_C(3)$; examples are shown in Fig. 1. In numerous UEDGE runs, we scan over different sets of amplitude factors to find those sets which give the best fits to available experimental data.

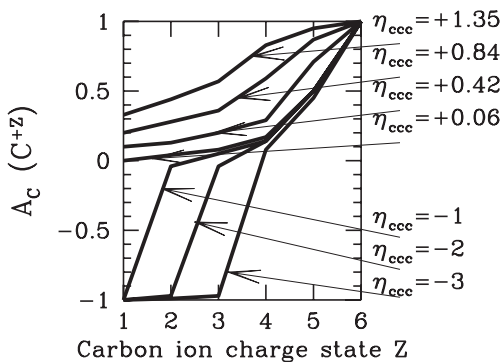


Fig. 1. Relative amplitude factors $A_C(Z)$ of carbon ion charge states C^{Z+} .

3. Results

In Ref. [4] we have analyzed the Simple-As-Possible-Plasma (SAPP) series of low-power L-mode shots on DIII-D and presented results of multi-ion UEDGE modeling for the lowest density shots (Nos. 105500-10, $\langle n_e \rangle \approx 2.4 \times 10^{13} \text{ cm}^{-3}$) in this series. Here, we present the results obtained for the higher density SAPP shots (Nos. 105517-19, $\langle n_e \rangle \approx 4.5 \times 10^{13} \text{ cm}^{-3}$) and focus on matching the impurity profile data. We use impurity data mainly from neutral-beam charge-exchange recombination (NB CER), filterscopes (FS), and a visible multi-chord divertor spectrometer (MDS). The arrangement of these diagnostics is shown in Fig. 2.

Based on plasma profiles calculated by UEDGE, the expected signals seen by the FS, MDS, and CER diagnostics are calculated from known view-cone geometries [6]. We use atomic physics data from ADAS. The effect of visible light reflections from the chamber interior walls on FS and MDS signals is estimated using the 3D ray-tracing routine [7,8] which incorporates the measured data [7] on visible light reflectance from the DIII-D carbon tiles.

The UEDGE solutions for shot 105517 are obtained with constant $D_{\perp} = 0.15 \text{ m}^2/\text{s}$, $\chi_{\perp} = 0.8 \text{ m}^2/\text{s}$ and with the SOL averaged values of convective velocity at the wall, $\langle V_{\text{BPconv}} \rangle \approx 90 \text{ m/s}$, and at the separatrix, $\langle V_{\text{BPconv}} \rangle \approx 2 \text{ m/s}$, by matching the following: particle flux balance at the core interface consistent with the NBI fueling rate, radial profiles of T_e and n_e measured in the SOL, mid-

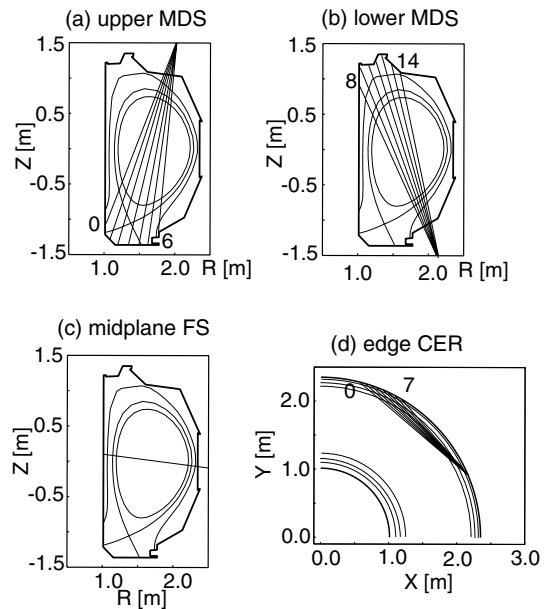


Fig. 2. Arrangement of impurity-relevant diagnostics in DIII-D.

plane gas pressure, divertor Thomson and Langmuir probe data, and D_α emission from divertor and main chamber (see Ref. [4], for the details). We use usual physical and chemical sputtering coefficients that follow those coefficients recently incorporated into the DIVIMP code [8]. As shown on Fig. 3, the obtained solutions are very sensitive to the impurity transport assumptions. The peak plasma temperature in the outer divertor T_{ed} , the relative concentration of C^{6+} in the core, $\xi_{C6} = [C^{6+}]/n_e$, and the brightness B_{mid} (C_{III}) of the C_{III} -ion line at 4650 Å seen by the horizontal mid-plane FS all depend strongly on the model parameter η_{CCC} . For $\eta_{CCC} < 0$, the inner divertor is predicted to be detached, in agreement with probe data and with D_α/D_α measurements in this region. Despite the detachment of inner divertor, the core plasma according to UEDGE prediction is fueled predominantly by recycling of neutral particles at the outer chamber wall. As seen on Fig. 3, reasonable agreement with experimental data is obtained for $-2 < \eta_{CCC} < -0.5$.

It is important to note that the same range for η_{CCC} was predicted in Ref. [4] for the lower density shot 105500. Moreover, the UEDGE simulation for the L-mode shot 105512 with intermediate discharge density $\langle n_e \rangle \approx 3.5 \times 10^{13} \text{ cm}^{-3}$ also gives a similar result. Then, all shots in the SAPP series have the same range $-2 < \eta_{CCC} < -0.5$ at which the experimental data on T_{ed} , ξ_{C6} , and B_{mid} (C_{III}) are well matched.

The beam charge-exchange recombination spectroscopy provides important information on the radial profile of density $[C^{6+}]$ of fully stripped carbon ions at the

mid-plane. As seen in Fig. 4, the C^{6+} density profile calculated by UEDGE matches the experiment reasonably well for $\eta_{CCC} < -1$, suggesting that low carbon ion charge states are convected inward. The core C^{6+} concentration is significantly underestimated in the case $\eta_{CCC} > 0$, when carbon ion charge states behave more like the main plasma species.

The brightness data measured along various MDS view-chords for the low charge states C_I , C_{II} , and C_{III} are shown in Fig. 5. The plotted lines show the UEDGE code predictions for the MDS data for different values of η_{CCC} . It can be seen that the brightness along divertor

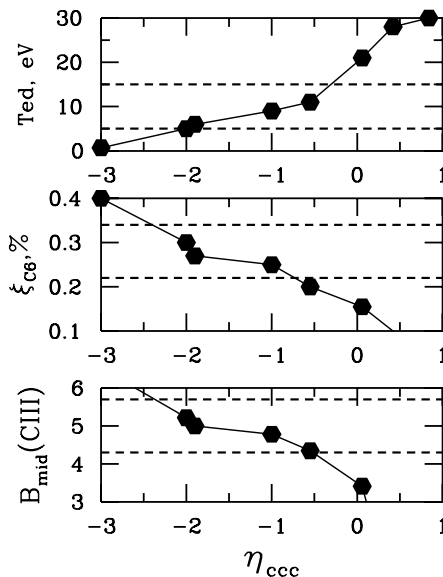


Fig. 3. Variation of T_{ed} , $\xi_{C6} = [C^{6+}]/n_e$, and B_{mid} with impurity model parameter η_{CCC} . On each panel, the experimental DIII-D data are scattered between two horizontal broken lines.

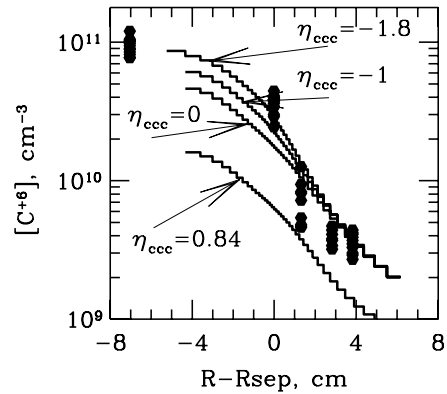


Fig. 4. The radial profiles of C^{6+} density calculated by UEDGE for a set of η_{CCC} values are compared to CER data (hexagons).

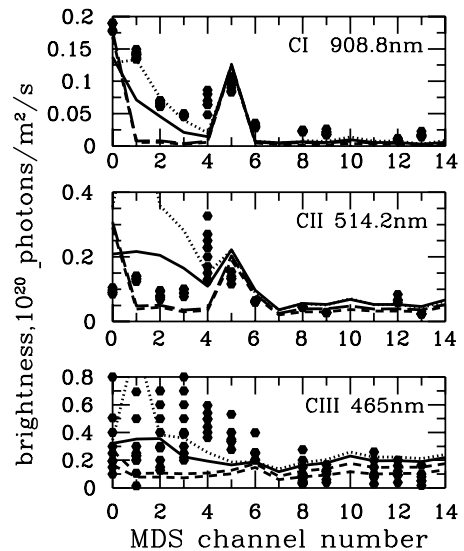


Fig. 5. MDS brightness measured and calculated for C_I , C_{II} , and C_{III} ions. See Fig. 2 for geometry of MDS channels (0–14). Lines connect data calculated by UEDGE for $\eta_{CCC} = -1.8$ (dotted line), $\eta_{CCC} = -1$ (solid), $\eta_{CCC} = 0$ (broken), and $\eta_{CCC} = 0.84$. Hexagons represent experimental data.

chords (MDS channels 0–6) changes weakly when η_{CCC} decreases from 0.84 to 0. For negative η_{CCC} values, the brightness of these chords varies strongly with η_{CCC} , as the inner divertor becomes detached. However, the calculations show that an increase in C_I , C_{II} , and C_{III} emission from the inner divertor region associated with detachment does not enhance substantially the carbon ion flux through the separatrix from inner divertor into the core. The upper MDS signals (channels 8–13) depend weakly on negative values of η_{CCC} , and the small increase in brightness is mainly due to the reflected light from the divertor region. For upper channels, the C_I and C_{II} brightness is dominantly from the impurities originating from walls. Note that view-cone of an MDS channel is very small and computed divertor emissions depend largely on EFIT equilibrium. Taking also into account the possible inaccuracy in ADAS atomic data, the uncertainty in chemical sputtering yield data, and the simplified assumptions on impurity atom transport in UEDGE, the best fit (within a factor 2) to MDS data for all ions gives the $\eta_{CCC} \approx -1$ for the SAPP shots with $\langle n_e \rangle \approx 4.5 \times 10^{13} \text{ cm}^{-3}$.

An important feature of SAPP series of shots is that the concentration of impurities in the core decreases with increasing discharge density $\langle n_e \rangle$, as shown on Fig. 6. In modeling of these discharges with AICFC model, the convective velocity $V_{BPconv}(w)$ near the outer wall is adjusted to match experimental data at the mid-plane, e.g., D_α brightness measured by the horizontal

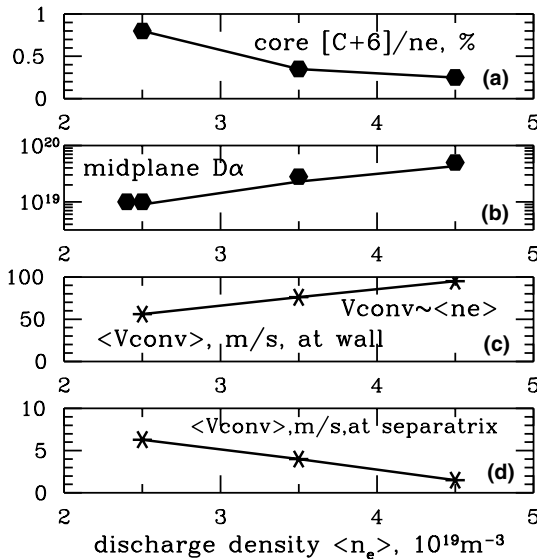


Fig. 6. Variation with L-mode SAPP discharge density of the following parameters calculated by UEDGE: C^{6+} concentration in the core (a), D_α brightness at the mid-plane FS (b), and averaged velocity V_{BPconv} at the wall (c) and at the separatrix (d). Hexagons represent experimental data.

FS. Since D_α -signals increase roughly as $\langle n_e \rangle^3$, the deduced $V_{BPconv}(w)$ increases almost linearly with $\langle n_e \rangle$. At the same time, the required $V_{BPconv}(s)$ inside the separatrix decreases with $\langle n_e \rangle$, mainly in response to increasing plasma opacity to neutrals. The decrease in $V_{BPconv}(s)$ reduces the scale for possible inward convection of impurities. We assume that the magnitude of inward convective velocity due to holes cannot exceed the magnitude of outward velocity due to blobs. Then, the reduced convective penetration of the carbon ions through the separatrix could decrease the core contamination. In addition, the ion temperature in the edge plasma reduces with increasing $\langle n_e \rangle$, so that the sputtering impurity source also decreases.

4. Conclusion

We apply the anomalous intermittent cross-field convection (AICFC) model to simulate the impurity transport within the framework of multi-fluid UEDGE code. As shown, this model improves the quality of the UEDGE simulations for extensive experimental DIII-D data.

The AICFC model introduces the amplitude factors (AF) for convective velocity of each charge state of impurity ion with respect to convective velocity of background ions. We find that UEDGE solutions are very sensitive to the values of amplitude factors. We test different sets of AF and find that the best fits to experimental data give the sets with parameter $-2 < \eta_{CCC} < -0.5$. These negative values of η_{CCC} correspond to the case when background ions and high charge state impurity ions are convected toward the wall, while the low charge state impurity ions either are convected inward, or have their outward convection substantially reduced compared to the background ions. The validated values of η_{CCC} are practically in the same range for all densities in L-mode shots. Moreover, in Ref. [5], the similar range for η_{CCC} was obtained for L-mode shots from NSTX and Alcator C-Mod tokamaks.

The present simulations do not include all capabilities of the UEDGE code. We intent to take the plasma \mathbf{ExB} and \mathbf{BxVB} drifts into account and to study carefully the combined effect of anomalous cross-field convection and macroscopic flows due to drifts on plasma and impurity transport in different tokamaks. For more realistic simulation of recycling neutral gas, we also plan to include molecules.

Acknowledgments

The work was performed under the auspices of the US Department of Energy by UCSD grant No. DE-FG02-04ER54739 and by University California LLNL

under contract No. W-7405-Eng-48. The originating developer of ADAS is the JET Joint Undertaking.

References

- [1] S.I. Krasheninnikov, *Phys. Lett. A* 283 (2001) 368.
- [2] D. D'Ippolito et al., *Contrib. Plasma Phys.* 44 (2004) 205.
- [3] T.D. Rognlien et al., *J. Nucl. Mater.* 196 (1992) 347.
- [4] A.Yu. Pigarov et al., *J. Nucl. Mater.* 313–316 (2003) 1076.
- [5] A.Yu. Pigarov et al., *Contrib. Plasma Phys.* 44 (2004) 228.
- [6] E.M. Hollmann, A.Yu. Pigarov, *Contrib. Plasma Phys.* 44 (2004) 301.
- [7] E.M. Hollmann, A.Yu. Pigarov, R.P. Doerner, *Rev. Sci. Instrum.* 74 (2003) 3984.
- [8] P.C. Stangeby, J. Elder, *J. Nucl. Mater.* 220–222 (1995) 193.